Available online at www.sciencedirect.com

ScienceDirect

Proceedings of the Combustion Institute 36 (2017) 737–744

Proceedings of the Combustion Institute

www.elsevier.com/locate/proci

Soot formation characteristics of diffusion flames of methane doped with toluene and *n*-heptane at elevated pressures

Adriana E. Daca, Ömer L. Gülder*

University of Toronto Institute for Aerospace Studies, 4925 Dufferin Street, Toronto, Ontario M3H 5T6, Canada

Received 28 November 2015; accepted 12 July 2016
Available online 25 July 2016

Abstract

Laminar co-flow diffusion flames of methane doped with *n*-heptane and toluene were studied experimentally to assess the sooting characteristics of two liquid fuels with increasing pressure. Experiments were conducted in the high-pressure combustion chamber that had been used previously for high-pressure soot formation studies in laminar diffusion flames. Either toluene or *n*-heptane was added to the methane such that 7.5% of the total carbon would be from the liquid fuel so that the results could be used to infer the pressure dependence of sooting propensities of the two liquid fuels. Pressure range was from atmospheric to 8 atm for methane and methane+*n*-heptane flames, whereas for methane+toluene mixture it was from atmospheric to 6 atm. A constant carbon mass flow rate of 0.41 mg/s for the three fuels was maintained at all pressures to have tractable measurements. Visible flame heights, as marked by the luminous soot radiation, were constant at all pressures except for methane at 1 atm. Variation of the maximum soot volume fractions, maximum soot yields, and the line-of-sight averaged soot temperatures of the three flames, pure methane, toluene-doped methane, and *n*-heptane-doped methane, with pressure were evaluated from soot spectral emission measurements which were collected line-of-sight but converted to radially-resolved values by using an Abel type inversion algorithm assuming axisymmetry of the laminar diffusion flames. Maximum soot volume fractions and maximum soot yields in *n*-heptane- and toluene-doped flames showed the higher sooting propensity of toluene in comparison to *n*-heptane at elevated pressures. Sooting propensity, in terms of both maximum soot yield and maximum soot volume fraction, of the methane+toulene flame displayed a relatively weaker dependence on pressure as compared to those of methane and methane+*n*-heptane mixture.

Keywords: High-pressure soot; Toluene; *n*-heptane; High-pressure laminar diffusion flames; Sooting propensity of liquid hydrocarbons

---

* Corresponding author.
E-mail addresses: ogulder@utias.utoronto.ca, flame-utias@usa.net (Ö.L. Gülder).

http://dx.doi.org/10.1016/j.proci.2016.07.046

1. Introduction

The sensitivity of soot processes to elevated pressures is important since most practical combustion devices operate at high pressures. The intensity of combustion (or heat release per unit volume) scales approximately with the square of the operating pressure, thus the footprint of the combustion engine becomes smaller as the operating pressure is increased for a required power output. On the other hand, the rate determining chemical reactions involved in combustion, including the various soot processes, are intrinsically nonlinear, and as a result the sensitivity of combustion events to pressure changes are not usually monotonic [1]. Therefore, it is not trivial to scale information gathered from measurements at atmospheric flames to high-pressure combustion.

For liquid fuels, we still rely on smoke point of the fuel or sooting index for practical applications due to a lack of full understanding of the effects of the various operating conditions on the soot formation process [2,3]. Earlier efforts to link the smoke point and sooting tendency of liquid fuels to chemical structure of the fuel were successful [4,5], and they provided scaling information for further studies on sooting propensities of hydrocarbons, see e.g., [6].

Information on soot formation processes in laminar diffusion flames at higher pressures is limited to ethylene [7–9], methane [7,10,11], ethane [12,13] and propane flames [14]. Data available on the sooting behavior of liquid fuels in tractable laminar diffusion flames at pressures above atmospheric are very limited; most data are at atmospheric pressure. A few studies with liquid fuels at pressures above atmospheric has been reported recently [3,15–18]. The effects of small amounts of *m*-xylene (up to 5% of fuel carbon coming from *m*-xylene as a perturbation to a base flame) on aromatic species and soot were studied in a nitrogen-diluted ethylene flame between 1 and 5 atm, Mensch et al. [3]. Their results indicate that the observed increase in soot and aromatic species are about first order with respect to amount of *m*-xylene added to the flame [3]. Karatas et al. [15] reported detailed measurements of soot volume fraction and temperature field in *n*-heptane diffusion flames diluted by nitrogen at pressures up to 7 atm. Comparing *n*-heptane results to ethylene flames, similarly diluted with nitrogen, revealed that *n*-heptane flame's soot yield is higher than that of ethylene at pressures above atmospheric [15]. Mouis et al. [16] investigated changes in soot volume fraction resulting from the addition of a JP-8 surrogate and each of its components to a nitrogen-diluted, ethylene co-flow diffusion flame between 1 and 5 atm. Pre-vaporized liquid fuel was added at two different levels: 2.5% and 5% of the total carbon flow rate. The linear behavior between the amount of carbon from the liquid fuel and the soot volume fraction suggests that the liquid fuel is not changing the base ethylene flame substantially [16]. Zhou et al. [17] studied the sooting behavior of *n*-heptane between 1 and 3 atm and inferred a pressure dependence of soot volume fraction similar to the one reported in [15]. However, the flame height, measured by luminescence and LII is reduced by 10% and 13%, respectively, from 1 atm to 3 atm. This indicates that the mass flow rate of *n*-heptane was not kept constant; so that the observed changes in sooting characteristics cannot be attributed to pressure change alone.

In this work we selected two liquid hydrocarbons, one paraffinic and one aromatic. Methane was used as the base fuel. Each liquid fuel was added to the base methane such that 7.5% of the carbon is provided by either *n*-heptane or toluene. Rationale for selecting methane as the base fuel is similar to the work reported by McEnally and Pfefferle [19] who doped methane flame with toluene such that it would account for 1.5% of the total fuel carbon flux in atmospheric diffusion flames. The main objective of the work reported here was to investigate the sooting behavior of co-flow methane laminar diffusion flames doped with *n*-heptane or toluene at pressures above atmospheric. Soot and temperature measurements in these flames at pressures from atmospheric to 8 atm are presented and discussed.

2. Experimental methodology

The laminar diffusion flame burner and the high-pressure combustion chamber used in this work have been described previously in detail [1,9,11–13,15]. A brief description, summarizing the essential features of the experimental set up, will be given here. The combustion chamber was designed to sustain pressures up to 110 atm and its internal diameter and height are 24 and 60 cm, respectively, Fig. 1. Optical access into the chamber is provided by three ports installed at 0°, 90°, and 180° permitting line-of-sight measurements as well as 90° imaging and scattering experiments. The chamber is mounted on a translational stage which is driven by three stepper motors that can move the chamber in three dimensions with a precision of 5 μm.

The burner used is a circular co-flow laminar diffusion type burner designed for liquid fuels and described in [15], and it is similar to those commonly used in high pressure soot studies [7,10]. The inner diameter of the burner at the exit is 3 mm and the outer diameter decreases gradually to a tapered fine edge to prevent any recirculation zones forming. The burner is manufactured from stainless steel and the burner tube has a metal foam insert to help to minimize the flow non-uniformities as well as providing heat transfer back to the liquid fuel vapor/methane mixture from the flame.

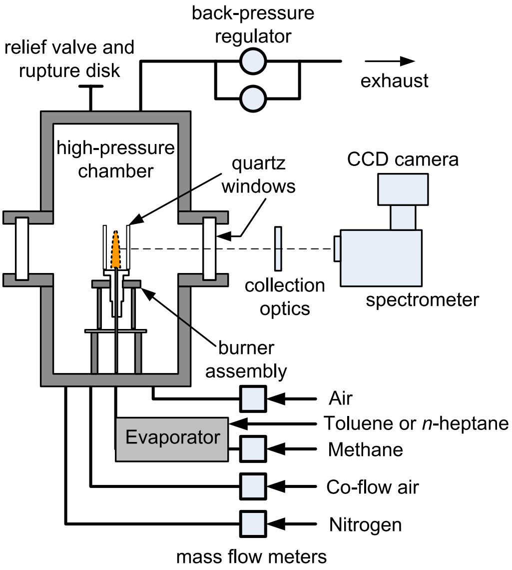

Fig. 1. A schematic view of the experimental setup.

The co-flow air nozzle is about 25 mm in diameter, and the air channel is fitted with the metal foam upstream of the burner exit to provide a tophat velocity profile [15].

The soot spectral emission technique was used to measure the soot concentration at different points in the flames as well as to estimate the temperature profiles of the flames [20]. Information from multiple wavelengths is required to resolve the soot concentration and temperature radially in an axisymmetric laminar diffusion flame using spectral emission [20]. The existing spectral emission setup at this laboratory consists of a spectrometer attached to a CCD camera. The radiation from the flame is focused into the spectrometer using an adjustable aperture in front of a lens. The spectrometer produces a spectrum of the radiation which is then recorded by the CCD camera as line-of-sight emission intensity. Further details of the soot spectral emission technique are documented in the literature [10,15,20].

All reactants, including liquid fuels, nitrogen, and compressed air, are of research grade purity. For gases, thermal mass flow controllers (Brooks SLA5850) were calibrated for the desired flow rates using a wet-bubble-cell calibration system (Sensidyne Gilibrator 2), which has accuracy traceable to NIST. A syringe pump (Teledyne), which controls the flow of liquid fuel, is connected to an evaporator and mixer unit (Bronkhorst), which is a system designed to provide controlled evaporation and flow of vapor mixtures. The temperature of the evaporator/mixer unit was set to its maximum of 200 °C and the fuel line temperature was set between 200 and 250 °C. The co-flow air was heated to 200 °C.

Table 1
Fuel and air flow rates for liquid fuel-doped methane experiments. f_{lc} = percentage of carbon from the liquid fuel; $\dot{m}_{CH_4}$ = methane mass flow rate; $\dot{m}_l$ = liquid fuel mass flow rate; $\dot{m}_a$ = co-flow air mass flow rate. Mass flow rates are in mg/s. Note that carbon mass flow rate in all cases is constant at 0.41 mg/s.

Fuel	f_{lc}	$\dot{m}_{CH_4}$	$\dot{m}_l$	$\dot{m}_a$
CH_4	0	0.55	0	340
CH_4/C_7H_{16}	7.5	0.51	0.036	340
CH_4/C_7H_8	7.5	0.51	0.033	340

Measurements were done by moving the chamber on its translational stage in 50 µm increments to complete a radial scan of the flame at a specific height and 1 mm increments along the flame axis. Knife-edge scans across a diffuse light source located at the object plane indicated a horizontal spatial resolution of 50 µm over the depth of field defined by the burner nozzle exit diameter. The vertical spatial resolution was inferred to be about 0.29 mm [15] At each measurement location, 3 images with an exposure time of 1 s were taken using the spectrometer attached to the CCD camera for gaseous fuels, and 5 images were taken at each location when measuring liquid fuel-doped flames, to gather emission intensity data required to estimate the soot temperature and concentration at each location. These line-of-sight measurements were then processed to construct radially-resolved soot volume fraction and temperature data for each height measured above the burner exit using a three-point Abel deconvolution algorithm.

One of the liquid fuels considered is *n*-heptane, and it is commonly used in surrogate mixtures for gasoline and diesel representing the alkane component of these fuels. Toluene was selected as the aromatic hydrocarbon, since it has the same carbon number as *n*-heptane, which allows a useful comparison of the difference in sooting propensity of alkanes and aromatics at elevated pressure. To have tractable flames, the carbon mass flow rates in methane, methane+*n*-heptane, and methane+toluene flames were identical and kept constant at all pressures, see Table 1.

Constant fuel mass flow rates ensure that the residence times are independent of pressure when compared at different heights within the flame. The premise of the experiments is that the results at a particular axial height above the burner exit are comparable for different pressures. This is based on the assumption that the height of a buoyancy-dominated laminar diffusion flame does not vary with pressure at a fixed fuel mass flow rate. Further, assuming equal residence times, this allows measurements from different pressures to be compared at the same height above the burner exit. The assumption of constant flame height with varying pressure is valid because the cross-sectional area

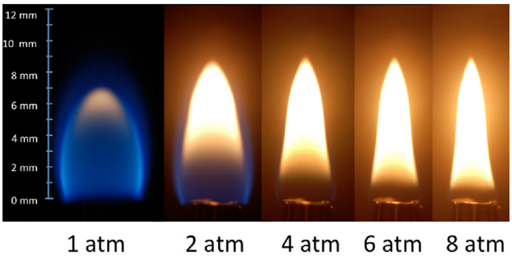

Fig. 2. Still pictures of the base fuel methane flames at various pressures.

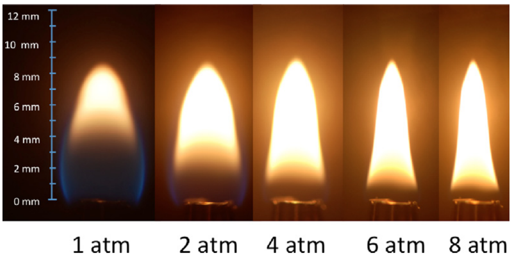

Fig. 3. Still pictures of the methane+*n*-heptane mixture flames at various pressures.

of the flame is inversely proportional to the pressure. As the pressure increases, the mass flow within the flame will be at a higher density, but through a smaller cross-section. Thus, at any given height above the burner, the same average velocity will be achieved [7,21]. The choice of pressures studied was limited by the maximum temperature of the evaporator/mixer unit and by the properties of the liquid fuels. The pressures at which the liquid fuels can be vaporized are limited by the temperature of the system and the vapor pressures of the fuels.

3. Results and discussion

As documented in the literature, the laminar co-flow diffusion flame shape changes with pressure and the characteristic flame cross-sectional area at a given location on the flame centerline scales with the inverse of pressure [1,12]. Still pictures of flames at various pressures, depicted in Figs. 2–4, display shapes similar to those observed previously at elevated pressures. In pure methane flames at atmospheric pressure, measurable soot concentrations are very low, however presence of soot clearly visible at pressures from 2 to 8 atm, Fig. 2. A qualitative comparison of the flames of methane+*n*-heptane, Fig. 3, and methane+toluene, Fig. 4, shows that at atmospheric pressure there is already appreciable soot in both flames; however, in the toluene-doped flame visible soot region is much larger than that of the *n*-heptane-doped flame.

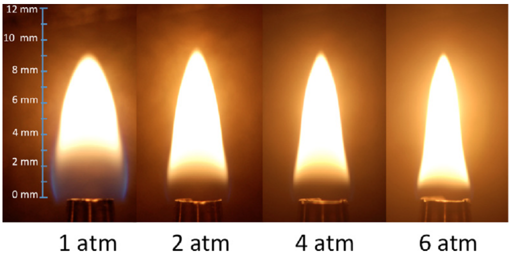

Fig. 4. Still pictures of the methane+toluene mixture flames at various pressures.

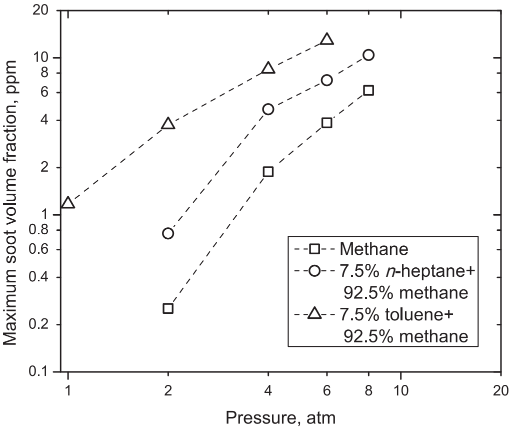

Fig. 5. Maximum soot volume fraction values of the three flames as a function of pressure.

For a quantitative comparison, maximum soot volume fractions of the three flames are shown in Fig. 5 as a function of pressure. Maximum soot volume fraction in base methane flame changes from 0.2 ppm at 2 atm to about 6 ppm at 8 atm, Fig. 5. Influence of 7.5% carbon from liquid fuels in methane on soot volume fractions is apparent in Fig. 5. In *n*-heptane-doped methane flame, maximum soot volume fraction increases from 0.8 ppm at 2atm to just over 10 ppm at 8 atm, whereas in toluene-doped methane flame maximum soot volume fraction is 4 ppm at 2 atm and about 13 ppm at 6 atm. Maximum soot volume fractions in *n*-heptane- and toluene-doped flames show the higher sooting propensity of an aromatic hydrocarbon in comparison to a normal paraffin with the same molecular carbon numbers. Pressure sensitivity of the maximum soot volume fraction in methane flame show a very similar behavior to ethane [12] and propane flames [14]. With the addition of *n*-heptane to methane the pressure sensitivity did not change significantly, Fig. 5; however, addition of toluene to methane seems to decrease the pressure dependence of the maximum soot volume fraction relative to methane.

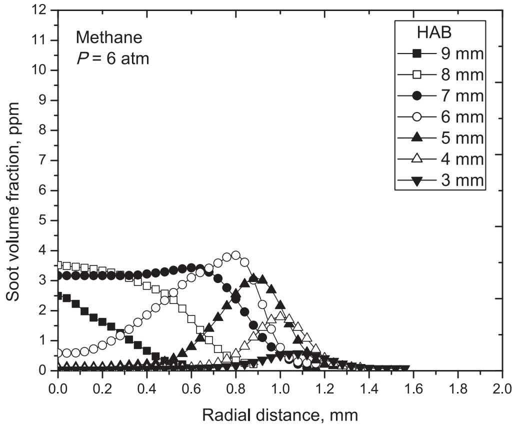

Fig. 6. Radially resolved soot volume fraction profiles of methane at 6 atm at various HAB locations.

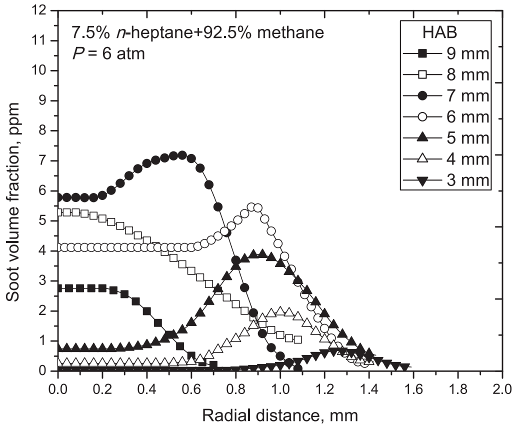

Fig. 7. Radially resolved soot volume fraction profiles of n-heptane doped methane flame at 6 atm at various HAB locations.

For a further comparison, radially resolved soot volume fractions at 6 atm pressure are shown in Figs. 6–8 for the three flames. Soot profiles display the characteristic shape of the soot volume fraction distributions with radial distance from the flame centreline and axial height in laminar co-flow diffusion flames. At 6 atm pressure, at 3 mm height above the burner maximum soot volume fraction is about 0.5 ppm in pure methane flame whereas it is close to 1 ppm in n-heptane-doped methane flame, Figs. 6 and 7. For the same conditions, toluene-doped flame produces soot close to 2 ppm, Fig. 8. The 3 mm axial height in these flames is in the region of the flame where the soot formation and growth processes are dominant. The influence of toluene on soot nucleation and growth is significant in spite of only 7.5% of the fuel stream's carbon is provided by toluene. At 5 mm, about mid-height of the flames, maximum soot volume fraction in methane flame is 3 ppm and it reaches 4 ppm in n-heptane-doped flame, whereas in toluene-doped flame it is about 6 ppm. The same order of soot volume fractions in three flames persist at higher heights than 5 mm above the burner.

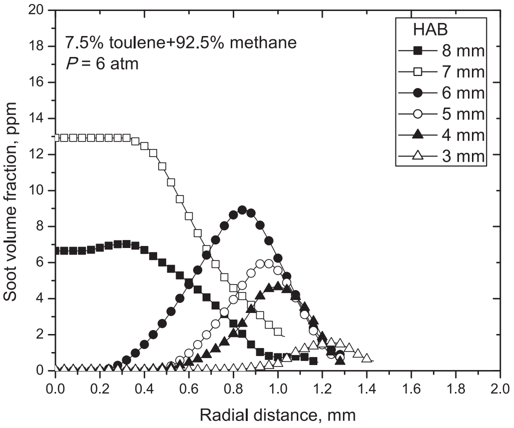

Fig. 8. Radially resolved soot volume fraction profiles of toluene doped methane flame at 6 atm at various HAB locations.

Direct comparison of soot volume fractions at different pressures could be misleading due to volume change with pressure. A more plausible way to assess the effect of pressure is to use the soot yield, which is the ratio of the mass of soot (assuming that soot consists of only carbon) at a given location in the flame to the total mass of carbon within the fuel. Mass flow rate of soot, $\dot{m}_s$, can be estimated at any axial flame cross-section from the soot volume fraction distribution and the velocity field within the flame as follows:

$$\dot{m}_s(z) = \rho_s \int 2\pi r f_v(r, z) v(r, z) dr \quad (1)$$

where v is the velocity, f_v is the soot volume fraction, and r and z are the radial and axial coordinates, respectively. An assumption implicit in Eq. (1) is that the soot mass density, ρ_s, is considered as constant throughout the flame, and it is taken as 1.8 g/cm^3 as was done in previous studies [10,11]. Extensive numerical simulations with similar flames indicated that $v(r, z)$ could be estimated fairly accurately from $(2az)^{1/2}$, where a is an acceleration constant approximated as $a \approx 41$ m/s^2 [13,22]. Soot yield, Y_s is given by

$$Y_s = \dot{m}_s(z)/\dot{m}_c \quad (2)$$

where $\dot{m}_c$ corresponds to the mass of carbon flow originating from the fuel at the nozzle exit. Mass flow rate of carbon was kept constant as 0.41 mg/s in this study. The maximum soot yields estimated by using Eqs. (1) and (2) are shown in Fig. 9 for the three flames as a function of pressure. Also shown in Fig. 9 are the soot yield data from a previous study with methane from 10 to 60 atm [11].

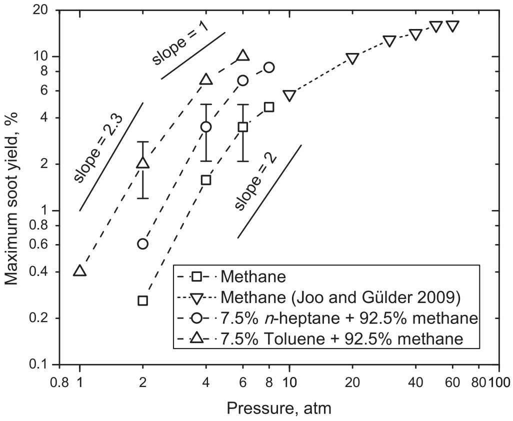

Fig. 9. Maximum soot yields of methane, methane+*n*-heptane, and methane+toluene flames at various pressures. Percentages reflect the percentage of carbon from each fuel. Methane data at pressures from 10 to 60 atm are from [11].

Response of the maximum soot yields to pressure seem similar for all these three flames considering the experimental uncertainties in estimating Y_s. At lower pressures, slopes of the soot yield curves are about 2.3–2.5 up to 4 atm for pure and *n*-heptane-doped flames and gradually decrease with increasing pressure (see guiding slope lines in Fig. 9). However, between 2 and 4 atm, slope for the flame doped with toluene is slightly lower than those for pure and *n*-heptane-doped methane flames. The decrease in the slope for toluene-doped flame continues between 4 and 6 atm; it is much lower than those for pure and *n*-heptane-doped methane flames. Unfortunately, it was not possible to have measurements at 8 atm with methane flame doped with toluene due to issues related to liquid fuel evaporation and flame stability.

The relatively weaker dependence on pressure of the maximum soot volume fraction and maximum soot yield with toluene-doped methane flame, in comparison with pure and *n*-heptane-doped methane flames, is unexpected. The only studies at elevated pressures with aromatic hydrocarbons related to soot were performed in shock tubes where soot forms either as a result of pyrolysis or in very rich premixed burning. Frenklach et al. [23] investigated soot formation in toluene-argon mixtures behind reflected shock waves over the temperature range of 1500–2300 K and the pressure range of 0.3 to 3 atm. Experimental data indicated that there is a strong pressure effect on soot formation within this pressure range. In a similar shock tube toluene pyrolysis experiment over a pressure range from 2.5 to 10 atm, a much smaller pressure effect on soot yield was observed [24,25]. These two sets of results from shock tube pyrolysis experiments with toluene indicate that the pressure sensitivity of soot yield of toluene pyrolysis is significant at pressures from 0.3 atm to 3 atm, whereas this effect is relatively weaker, or “little quantitative effect” as described by the authors [25], at pressures between 2.5 and 10 atm. This trend in pressure effect in toluene pyrolysis support our observations of soot yield in toluene-doped methane flames showing a relatively weaker pressure effect as compared to methane and *n*-heptane-doped methane flames. A similar trend was observed in the pyrolysis of benzene in shock tube experiments [26,27]. Two major decomposition routes for toluene have been proposed; namely, removal of an H atom from the methyl side-chain to form benzyl radical and complete removal of the side-chain to form phenyl radical [19]. The latter route is also one of the decomposition channels in benzene pyrolysis. Between 6 and 60 atm, soot yield of benzene in shock tube pyrolysis experiments did not change significantly [26,27] indicating relatively weak or negligible pressure dependence of soot yields of simple aromatic hydrocarbons.

There is experimental evidence that toluene inhibits the pyrolysis of alkanes, although at much lower temperatures, between 625–875 K at low pressures [28]. It is not known whether this inhibition would be in effect in toluene-methane mixtures at much higher temperatures involved in flames. Experimental data from laminar diffusion flames above 6 atm are desirable to assess fully the pressure dependence of sooting propensity of the aromatic hydrocarbons like toluene.

In shock tube studies with rich premixed combustion of methane and *n*-heptane, Kellerer et al. [29] found a significant dependence of soot yield on pressure up to 30 atm; above 30 atm, the pressure seemed to lose its dominance. Between 1 and 7 atm, in nitrogen-diluted *n*-heptane flames the pressure effect on soot yield was found to be similar to gaseous hydrocarbons [15]. Although our findings with *n*-heptane-doped methane flames generally support these two previous studies [15,29], the sooting propensity of methane+*n*-heptane mixture increases slightly faster than that of pure methane between 4 and 8 atm with increasing pressure, Fig. 9. It is difficult to assess whether adding small amounts of *n*-heptane to methane would trigger a synergistic effect that would contribute to the amount of soot formed. Roesler et al. [30] studied methane+*n*-heptane mixtures in atmospheric coflow laminar diffusion flames and they uncovered synergistic effects caused by large amounts of CH_3 radical generated by the pyrolysis of methane; however, the contribution of this effect on soot volume fraction was found to be negligible in spite of a larger contribution to PAH formation, because of a compensating reduction in surface growth from acetylene [30].

Characteristic flame temperature profiles, evaluated as the integrated values over the flame diameter (i.e., the line-of-sight temperature) at a given height above the burner are shown in Fig. 10 at 2

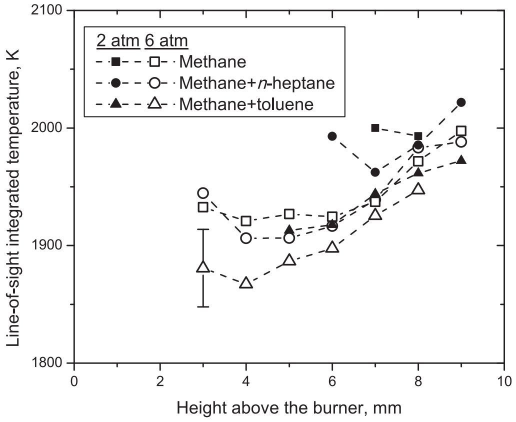

Fig. 10. Line-of-sight emission averaged soot temperature along the flame axis as a function of flame axial locations at 2 and 6 atm for the three flames.

and 6 atm. Overall trend is that the line-of-sight averaged flame temperature of methane+toluene is lowest and that of pure methane is the highest at both pressures, Fig. 10. Although the changes in flame temperature of methane would be minimal because of small amounts of liquid fuels added, a few degrees of temperature increase would be expected under ideal circumstances. However, heat loss from the flames as a result of soot radiation changes the picture. Higher soot loading leads to lower flame temperatures. It would be speculative to assess the effect of lowered flame temperatures on soot formation rates with the current data. But, lower temperatures are expected to slow down soot processes, such as nucleation, coalescence, and surface growth as well as soot oxidation [31,32]. If it were possible to keep the flame temperatures identical, then the soot yields of methane+*n*-heptane and methane+toluene would be expected to be slightly higher than those shown in Fig. 9.

The maximum total uncertainty related to soot measurements in this work was evaluated as 40%. The total uncertainty in temperature measurements by the spectral soot emission technique was estimated as 3.5%. It should be noted that a major part of the uncertainties, more than 70–80%, is due to systematic errors mostly originating from the uncertainty in the soot refractive index. Systematic errors, as the name implies, are consistent in direction and by a scale factor, so they do not influence the observed trend in data comparisons. In view of the magnitude of the uncertainty due to random errors, observed data trends are statistically sound and conclusions based on these data are reliable. The error bars in Figs. 9 and 10 correspond to these maximum total uncertainties.These uncertainties are similar to those estimated for our previous studies using the same measurement techniques with gaseous and liquid fuel diffusion flames at high pressures [8,10–12,14,15]. Full details of the methodologies for the uncertainty analysis can be found in [20,33].

4. Conclusions

Effects of pressure on sooting propensities of two liquid hydrocarbons with the same number of carbon atoms but different chemical structures, namely *n*-heptane and toluene, were studied in laminar diffusion flames at high pressures. Liquid hydrocarbons were added to the base fuel methane in amounts to have 7.5% of total carbon to be contributed from either toluene or *n*-heptane. Pressure range was from atmospheric to 8 atm for methane and methane+*n*-heptane flames, whereas for methane+toluene mixtures it was from atmospheric to 6 atm. A constant carbon mass flow rate of 0.41 mg/s for the three fuels, pure methane, methane+*n*-heptane and methane+toluene, was maintained at all pressures to have tractable measurements. Constant mass flow rate of fuels resulted in constant visible flame heights, as marked by the luminous soot radiation, at all pressures except for methane flame at 1 atm. Experimental data were collected using soot spectral emission technique in the high-pressure combustion chamber that had been used previously for high-pressure soot formation studies in laminar diffusion flames. Line-of-sight emission data were inverted using Abel inversion to obtain radially resolved temperatures and soot volume fractions assuming axisymmetry of the laminar diffusion flames. From radially resolved soot volume fractions, soot yields were evaluated. Comparison of the maximum soot volume fractions and soot yields of the two liquid hydrocarbons, that were added to methane, indicated a much higher sooting propensity of toluene relative to *n*-heptane at pressures considered. Sooting propensity, in terms of both maximum soot yield and maximum soot volume fraction, of the methane+toluene mixture indicated a relatively weaker dependence on pressure as compared to methane and methane+*n*-heptane. It was argued that this is probably a consequence of very weak pressure effects in soot formation in benzene and toluene pyrolysis at pressures above 2–3 atm.

Acknowledgments

The financial support was provided by the Natural Sciences and Engineering Research Council of Canada through discovery (251116-2012) and strategic project (STPGP 430362-12) grants, and by the BioFuelNet Canada (7B_Gulder).

References

[1] A.E. Karataş, Ö.L. Gülder, *Prog. Energy Combust. Sci.* 38 (2012) 818–845.

[2] D.B. Olson, J.C. Pickens, R.J. Gill, *Combust. Flame* 62 (1985) 43–60.

[3] A. Mensch, R. Santoro, T.A. Litzinger, S.-Y. Lee, *Combust. Flame* 157 (2010) 1097–1105.

[4] R.A. Hunt, *Ind. Eng. Chem.* 45 (1953) 602–606.

[5] O.L. Gülder, *Combust. Flame* 78 (1989) 179–194.

[6] L. Li, P.B. Sunderland, *Combust. Sci. Technol.* 184 (2012) 829–841.

[7] L.L. McCrain, W.L. Roberts, *Combust. Flame* 140 (2005) 60–69.

[8] H. Joo, Ö.L. Gülder, *Combust. Flame* 158 (2011) 416–422.

[9] A.E. Karataş, Ö.L. Gülder, *Combust. Flame* 162 (2015) 1566–1574.

[10] K.A. Thomson, Ö.L. Gülder, R.A. Weckman, E.J. Fraser, G.J. Smallwood, D.R. Snelling, *Combust. Flame* 140 (2005) 222–232.

[11] H.I. Joo, Ö.L. Gülder, *Proc. Combust. Inst.* 32 (2009) 769–775.

[12] P.M. Mandatori, Ö.L. Gülder, *Proc. Combust. Inst.* 33 (2011) 577–584.

[13] Ö.L. Gülder, G. Intasopa, H.I. Joo, P.M. Mandatori, D.S. Bento, M.E. Vaillancourt, *Combust. Flame* 158 (2011) 2037–2044.

[14] D.S. Bento, K.A. Thomson, Ö.L. Gülder, *Combust. Flame* 145 (2006) 765–778.

[15] A.E. Karatas, G. Intasopa, Ö.L. Gülder, *Combust. Flame* 160 (2013) 1650–1656.

[16] A.G. Mouis, T.A. Litzinger, Y. Wang, et al., *Combust. Flame* 162 (2015) 1987–1995.

[17] L. Zhou, N.J. Dam, M.D. Boot, L.P.H. de Goey, *Combust. Flame* 160 (2013) 2507–2516.

[18] L. Zhou, N.J. Dam, M.D. Boot, L.P.H. de Goey, *Combust. Flame* 161 (2014) 2669–2677.

[19] C.S. McEnally, L.D. Pfefferle, *Combust. Sci. Technol.* 128 (1997) 257–278.

[20] D. Snelling, K. Thompson, G. Smallwood, Ö.L. Gülder, *AAIA J.* 40 (2002) 1789–1795.

[21] I. Glassman, R.A. Yetter, *Combustion*, Academic Press, 2008.

[22] M.R.J. Charest, H.I. Joo, Ö.L. Gülder, C.P.T. Groth, *Proc. Combust. Inst.* 33 (2011) 549–557.

[23] M. Frenklach, S. Taki, R.A. Matula, *Combust. Flame* 49 (1983) 275–282.

[24] T.S. Wang, *Soot formation from toluene,* Ph.D. thesis, Loussianna State University, 1980.

[25] T.S. Wang, R.A. Matula, R.C. Farmer, *Proc. Combust. Inst.* 18 (1981) 1149–1158.

[26] Y.G. Knorre, D. Tanke, T. Thienel, H.G. Wagner, *Proc. Combust. Inst.* 26 (1996) 2303–2310.

[27] D. Tanke, *Russbildung in der Kohlenwasserstoffpyrolyse hinter Stosswellen,* Ph.D. thesis, Georg-August-Universität zu Göttingen, 1994.

[28] F. Lannuzel, R. Bounaceur, R. Michels, G. Scacchi, P.-M. Marquaire, *Energy Fuels* 24 (2010) 3817–3830.

[29] H. Kellerer, A. Müller, H.J. Bauer, S. Wittig, *Combust. Sci. Technol.* 113–114 (1996) 67–80.

[30] J. Roesler, S. Martinot, C. McEnally, L. Pfefferle, J.-L. Delfau, C. Vovelle, *Combust. Flame* 134 (2003) 249–260.

[31] Ö.L. Gülder, *Combust. Flame* 88 (1992) 75–82.

[32] Ö.L. Gülder, D.R. Snelling, *Combust. Flame* 92 (1993) 115–124.

[33] K.A. Thomson, *Soot Formation in Annular Non-premixed Laminar Flames of Methane-air at Pressures of 0.1 to 4.0 MPa,* Ph.D. thesis, University of Waterloo, 2004.